Photoinduced Processes in Dyads and Triads: An Osmium(II)–Bis(terpyridine) Photosensitizer Covalently Linked to Electron Donor and Acceptor Groups

Jean-Paul Collin,[1a] **Stephane Guillerez,**[1a] **Jean-Pierre Sauvage,**[1a] **Francesco Barigelletti,***[,1b] **Luisa De Cola,**[1c] **Lucia Flamigni,**[1b] **and Vincenzo Balzani**[1c]

Laboratoire de Chimie Organo-Minerale, Institut de Chimie, Université Louis Pasteur,
F-67000 Strasbourg, France, and Istituto FRAE-CNR and Dipartimento di Chimica
"G. Ciamician" dell'Università, 40126 Bologna, Italy

Received October 7, 1991

We have synthesized the luminescent $Os(ttp)_2^{2+}$ photosensitizer (P) and the supramolecular species P–A, D–P, and D–P–A where the photosensitizer is covalently linked to the electron acceptor MV^{2+} (A) and/or the electron donors PTZ or DPAA (D); ttp is 4′-(*p*-tolyl)-2,2′:6′,2″-terpyridine, MV^{2+} is methylviologen, PTZ is phenothiazine, and DPAA is di-*p*-anisylamine. The absorption spectra, emission spectra and lifetimes in the nano- and picosecond time scales (in the 90–298 K temperature range), nanosecond transient absorption spectra and lifetimes (at 155 and 298 K), and the electrochemical behavior of the P, P–A, D–P, and D–P–A species have been investigated in acetonitrile or butyronitrile solutions. The main results can be summarized as follows: (i) the excited photosensitizer *P displays luminescence and decays with τ = 540 and 220 ns at 155 and 298 K respectively; (ii) the behavior of the D–P dyads, whose D^+–P^- charge-separated state lies at higher energy than the luminescent D–*P level, is essentially the same as that of P; (iii) in the P–A dyad, whose P^+–A^- charge-separated level lies at lower energy than the *P–A luminescent level, the luminescence intensity of the photosensitizer reduces to 1.9% and exhibits a lifetime of 4 ns at 155 K (260 ps at 298 K); the decay of the charge-separated species occurs with lifetime 27 ns and < 10 ns at 155 and 298 K respectively; (iv) the D–P–A triad with D = PTZ behaves essentially as the P–A dyad; (v) for the D–P–A triad with D = DPPA, the luminescence intensity reduces to ~1% at 298 K (τ = 190 ps). No direct evidence is obtained for the presence and survival of the fully charge-separated state D^+–P–A^-. In a rigid matrix at 77 and 90 K, no quenching of the luminescence can be observed in all the dyads and triads examined.

Introduction

There is much current interest in the design and study of supramolecular model species (dyads, triads, etc.) capable of mimicking the photoinduced charge separation processes that occur in photosynthetic reaction centers.[2-10] The key factors that determine the rates of forward and back electron transfer are energetics, solvent, nature of the connecting groups (spacers), and distance and relative orientation of the interacting partners.

As pointed out previously,[11,12] the bis-trpy metal complexes (trpy = 2,2′:6′,2″-terpyridine) that can play the role of photosensitizers (P) offer the possibility to design D–P–A triads where the donor (D) and acceptor (A) groups are linked in opposite positions with respect to the photosensitizer (trans-type configuration). In addition, bis-trpy complexes bearing substituents at the 4′-position do not lead to isomeric (enantio- and diasteromeric) mixtures, contrary to their equivalent substituted tris-bpy systems. Therefore, interposition of the aromatic rings (Figure 1) affords a very convenient way to increase the A–D separation distance.[11]

In a previous paper[12] we investigated the behavior of the $Ru(ttp)_2^{2+}$ photosensitizer (P) covalently linked to the MV^{2+} electron acceptor (A) and/or the PTZ or DPPA electron donors (D); ttp is 4′-(*p*-tolyl)-2,2′:6′,2″-terpyridine, MV^{2+} is methyl viologen, PTZ is phenothiazine, and DPAA is di-*p*-anisylamine. A limitation in that study was the very short lifetime and the lack of luminescence of $Ru(ttp)_2^{2+}$ at room temperature, which forced us to work in the temperature range below 200 K. In this paper we have investigated the analogous systems based on the $Os(ttp)_2^{2+}$ photosensitizer, whose lowest excited state is relatively long-lived (220 ns) and is luminescent in acetonitrile solution at room temperature. Investigations have therefore been performed at room temperature as well as at low temperature. Other important differences between the Ru and Os complexes, of course, concern the excited-state energy and the redox potentials.

In the present study, equipment for time-resolved emission spectroscopy with picosecond resolution, recently developed in our laboratories, has also been used.

The systems studied are illustrated in Figure 1, where the abbreviations used and the way in which we have "subdivided" the various supramolecular structures into molecular components are also shown.[13] The edge-to-edge distance between X and Y components is 21 Å.

---

[1] (a) Université de Strasbourg. (b) Istituto FRAE-CNR. (c) Università di Bologna.

[2] It would be impossible to give an exhaustive list of original papers on this subject. For recent reviews and articles of general interest, see refs 3–10.

[3] (a) Oevering, H.; Paddon-Row, M. N.; Heppener, M.; Oliver, A. M.; Cotsaris, E.; Verhoeven, J. W.; Hush, N. S. *J. Am. Chem. Soc.* **1987**, *109*, 3258. (b) Antolovich, M.; Keyte, P. J.; Oliver, A. M.; Paddon-Row, M. N.; Kroon, J.; Verhoeven, J. W.; Jonker, S. A.; Warman, J. M. *J. Phys. Chem.* **1991**, *95*, 1933.

[4] Closs, G. L.; Miller, J. R. *Science* **1988**, *240*, 440.

[5] Connolly, J. S.; Bolton, J. R. In *Photoinduced Electron Transfer, Part D*; Fox, M. A., Chanon, M., Eds.; Elsevier: Amsterdam, 1988, p 303.

[6] (a) Wasielewski, M. R. In *Photoinduced Electron Transfer, Part A*; Fox, M. A., Chanon, M., Eds.; Elsevier: Amsterdam, 1988; p 161. (b) Gaines, G. L., III; O'Neil, M. P.; Svec, W. A.; Niemczyk, M. P.; Wasielewski, M. R. *J. Am. Chem. Soc.* **1991**, *113*, 719.

[7] Gust, D.; Moore, T. A., Eds.; *Tetrahedron* **1989**, *45*, 4669–4903.

[8] Meyer, T. J. *Acc. Chem. Res.* **1989**, *22*, 163.

[9] Scandola, F.; Indelli, M. T.; Chiorboli, C.; Bignozzi, C. A. *Top. Curr. Chem.* **1990**, *158*, 73.

[10] Balzani, V.; Scandola, F. *Supramolecular Photochemistry*; Horwood: Chichester, U.K., 1991; Chapter 5.

[11] Collin, J.-P.; Guillerez, S.; Sauvage, J.-P. *J. Chem. Soc., Chem. Commun.* **1989**, 776.

[12] Collin, J.-P.; Guillerez, S.; Sauvage, J.-P.; Barigelletti, F.; De Cola, L.; Flamigni, L.; Balzani, V. *Inorg. Chem.* **1991**, *30*, 4230.

[13] As discussed elsewhere,[10,12] in covalently-linked multicomponent systems there are nomenclature problems related to the fact that covalent linking implies more or less small modifications of the isolated molecular species. For example, 4′-(*p*-tolyl)-2,2′:6′,2″-terpyridine and its abbreviation, ttp, are right when used for the ligands of the isolated photosensitizer

0020-1669/92/1331-4112$03.00/0

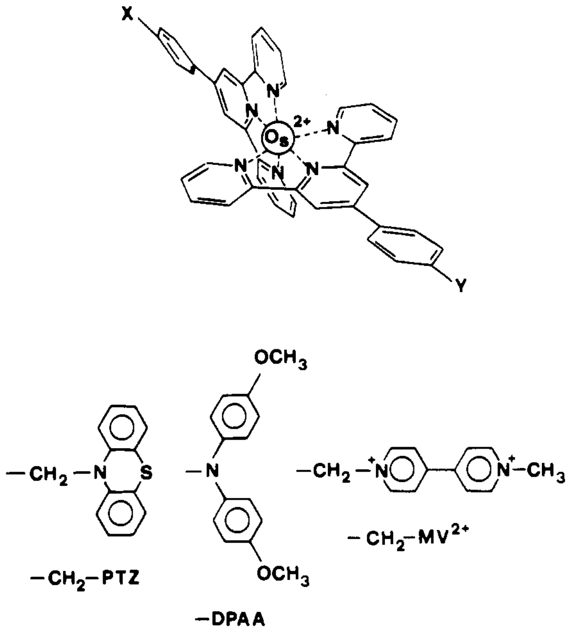

Figure 1. Illustration of the investigated systems and abbreviations used: X = $-CH_3$ and Y = $-CH_3$, $Os(ttp)_2^{2+}$ photosensitizer, P; for X = $-CH_3$ and Y = $-MV^{2+}$, P–A photosensitizer–acceptor dyad, $Os(ttp)_2^{2+}$–MV^{2+}; for X = $-CH_2$–PTZ or -DPAA and Y = $-CH_3$, D–P donor–photosensitizer dyads, PTZ–$Os(ttp)_2^{2+}$ and DPAA–$Os(ttp)_2^{2+}$; for X = $-CH_2$–PTZ or -DPAA, Y = $-MV^{2+}$, D–P–A donor–photosensitizer–acceptor triads, PTZ–$Os(ttp)_2^{2+}$–MV^{2+} and DPAA–$Os(ttp)_2^{2+}$–MV^{2+}.

Experimental Section

Instrumentation and Procedures. The instruments and procedures used to obtain ^1H NMR spectra, mass spectra, melting points, elemental analyses, cyclic voltammograms, ground-state absorption spectra, luminescence spectra, transient absorption spectra and decays, and luminescent decays in the nanosecond time scale have been described in a previous paper.[12] The detection of luminescence decays in the picosecond time scale was based on a Nd-YAG laser, a spectrograph, and a streak camera. The laser (Continuum PY62-10) is a cavity dumped, actively/passively mode-locked Nd:YAG with two amplification stages, delivering pulses of 35 ps, with repetition rates variable up to 10 Hz and energy up to 120 mJ/pulse at 1064 nm. The second harmonic (532 nm), with an energy of 0.5 mJ/pulse, was used to excite the sample (A_{532} = 1.0). The light emitted by the sample was collected at the right angle via a system of lenses and fed into the entrance slit of a spectrograph (HR 250 Jobin-Yvon). The light, horizontally dispersed by the spectrograph, entered the slit (20 μm) of the streak camera (Hamamatsu C1587) equipped with a Model M1952 fast single sweep unit with 2-ps resolution. Acquisition and processing of the data were obtained via a Hamamatsu Microlux system consisting of a cooled CCD camera (C3140), related software, and a Compaq 386 PC computer. Typical signals of intensity vs time in the 730–750-nm wavelength range were obtained by integration over 1000 laser shots. Overall time resolution including triggering jitter is 15 ps. The analysis performed with standard iterative nonlinear deconvolution procedure gave single exponentials.

Chemical shifts of NMR spectra are reported referenced to Me_4Si as an internal standard. Electrochemical potentials are reported vs SSCE. The experiments were carried out in freshly distilled acetonitrile or butyronitrile. For the photochemical and photophysical experiments, dilute (10^{-4}–10^{-5} M) solutions of the samples were sealed under vacuum in 1-cm quartz cells after repeated freeze–pump–thaw cycles. Luminescence quantum yields in degassed solution at room temperature were measured, following the procedure indicated by Parker and Rees,[14] using $Os(bpy)_3(PF_6)_2$ in acetonitrile as a standard (Φ = 0.0050 at 298 K[15]). The uncertainties on the reported measurements of emission maxima and emission quantum yields are estimated to be ±2 nm and ±20%, respectively. The uncertainty in the luminescence lifetimes is ±8%. The instrument resolution for the single photon counting equipment[12] is 0.2 ns, and that for the picosecond experiments is 15 ps. The instrument resolution for the transient absorption experiments was 20 ns, and the uncertainty in the lifetimes is ±10%.

Chemicals. High-purity commercial reagent grade products were used without purification. The ligands ttp, ttp–MV^{2+}, ttp–PTZ, and ttp–DPAA and the complexes $Os(ttp)_2^{2+}$, $[Os(ttp)_2–MV]^{4+}$, $[PTZ–Os(ttp)_2]^{2+}$, and $[DPAA–Os(ttp)_2]^{2+}$ were prepared as described previously.[11,12,16] The purification of all osmium complexes was performed on chromatography columns protected from light.

Preparation of $[PTZ–Os(ttp)_2–MV](PF_6)_4$ and $[DPPA–Os(ttp)_2–MV](PF_6)_4$. The common intermediate of these triads, $[Os(ttp–MV)(O)_2(OH)](BF_4)_3$, was synthesized by the same method as $[Os(ttp)(O)_2(OH)](NO_3)$.[16] A THF/H_2O (10:30 cm³) solution of $[Os(ttp–MV)(O)_2(OH)](BF_4)_3$ (0.213 g, 0.21 mmol) was added dropwise, under argon, to a THF/H_2O (35:15 cm³) mixture containing 0.21 mmol of ligand (ttp–PTZ or ttp–DPAA) and 0.25 cm³ of hydrazine hydrate (5.1 mmol). The reaction mixture was stirred under reflux for 10 min, and the THF was then evaporated. The brown solution was treated with 0.5 g of KPF_6. The precipitate obtained was washed with water (100 cm³) and toluene (200 cm³). The product was purified by silica gel chromatography, eluting with $CH_3CN–H_2O$ mixtures containing KNO_3 (85:15 to 60:40; $[KNO_3]$ = 0.08–0.4 M).

$[PTZ–Os(ttp)_2–MV](PF_6)_4$. Yield: 2%. δ_H (CD_3CN): 9.13 (d, 2 H, 6.6 Hz); 9.02 (s, 2 H); 9.01 (s, 2 H); 8.88 (d, 2 H, 6.5 Hz); 8.64 (d, 2 H, 4.3 Hz); 8.60 (d, 4 H, 4.2 Hz); 8.50 (d, 2 H, 6.5 Hz); 8.42 (d, 2 H, 6.8 Hz); 8.29 (d, 2 H, 8.2 Hz); 8.14 (d, 2 H, 8.3 Hz); 7.87–7.74 (m, 8 H); 7.31–6.92 (m, 16 H); 6.02 (s, 2 H); 5.37 (s, 2 H); 4.42 (s, 3 H). FABMS (nitrobenzyl alcohol matrix), *m/z*: 1640.0; $[PTZ–Os(ttp)_2–MV](PF_6)_3^+$ requires *m/z* 1640.

$[DPAA–Os(ttp)_2–MV](PF_6)_4$. Yield: 7%. δ_H (CD_3CN): 9.11 (d, 2 H, 7.1 Hz); 9.00 (s, 2 H); 8.96 (s, 2 H); 8.88 (d, 2 H, 6.7 Hz); 8.64–8.57 (m, 4 H); 8.49 (d, 2 H, 7.1 Hz); 8.41 (d, 2 H, 6.8 Hz); 8.28 (d, 2 H, 8.4 Hz); 8.00 (d, 2 H, 8.9 Hz); 7.86–7.75 (m, 6 H); 7.43 (d, 2 H, 5.6 Hz); 7.23 (d, 4 H, 9.0 Hz); 7.01 (d, 4 H, 9.0 Hz); 7.25–6.99 (m, 8 H); 6.02 (s, 2 H); 4.42 (s, 3 H); 3.88 (s, 6 H). FABMS (nitrobenzyl alcohol matrix), *m/z*: 1656.2; $[DPA–Os(ttp)_2–MV](PF_6)_3^+$ requires *m/z* 1656.

Results

Stability. The employed solvents were freshly distilled because of partial decomposition of the supramolecular species in aged solvents. All the compounds studied were stable under the conditions used, sealed under vacuum, both in the dark and upon excitation with visible light. In particular, no changes in the absorption and luminescence properties have been found after prolonged irradiation of sealed acetonitrile and butyronitrile solutions of P–MV^{2+} and DPAA–MV^{2+} with visible light. An upper limiting value for the photodecomposition quantum yield is estimated to be 10^{-4}.

Electrochemistry. The electrochemical waves of the dyads and triads (Table I) can easily be assigned by comparison with the waves observed for the isolated components.[15,17–20] For illustration purposes, the cyclic voltammogram for the PTZ-$Os(ttp)_2^{2+}$-MV^{2+} triad is presented in Figure 2.

Ground-State Absorption Spectra. The absorption spectrum of $Os(ttp)_2^{2+}$ is characterized by intense bands in the UV and visible regions (Table II). The bands centered at about 286 and 314 nm correspond to ligand-centered (^{1}LC) transitions, while those in the visible region correspond to Os → ttp metal-to-ligand charge transfer transitions (^{1}CT, 490 nm; ^{3}CT, 667 nm).[17,21] The

---

$Os(ttp)_2^{2+}$ but are not correct when applied to the photosensitizer component of a dyad and triad. It is however preferable to maintain the same abbreviations for the free and covalently linked components in order to better understand the chemical parentage of the various systems investigated.

(14) Parker, C. A.; Rees, W. T. *Analyst (London)* **1960**, *85*, 587.

(15) Kober, E. M.; Caspar, J. V.; Lumpkin, R. S.; Meyer, T. J. *J. Phys. Chem.* **1986**, *90*, 3722.

(16) Collin, J.-P.; Guillerez, S.; Sauvage, J.-P. *Inorg. Chem.* **1990**, *29*, 5009.

(17) (a) Meyer, T. J. *Pure Appl. Chem.* **1986**, *58*, 1193. (b) Kober, E. M.; Caspar, J. W.; Sullivan, B. P.; Meyer, T. J. *Inorg. Chem.* **1988**, *27*, 4587. (c) Della Ciana, L.; Dressick, W. J.; Sandrini, D.; Maestri, M.; Ciano, M. *Inorg. Chem.* **1990**, *29*, 2792.

(18) Hünig, S.; Grass, J.; Schenk, W. *Liebigs Ann. Chem.* **1973**, 324.

(19) Billon, J.-P. *Ann. Chim.* **1962**, *7*, 183.

(20) Seo, E. T.; Nelson, R. F.; Fritsch, J. M.; Marcoux, L. S.; Leedy, D. W.; Adams, R. N. *J. Am. Chem. Soc.* **1966**, *88*, 3498.

(21) Stone, M. L.; Crosby, G. A. *Chem. Phys. Lett.* **1981**, *79*, 169.

Table I. Electrochemical Potentials and Their Assignments[a]

	Os^{3+}/Os^{2+}	$DPAA^{+/0}$	$PTZ^{+/0}$	$MV^{2+/+}$	ttp/ttp$^-$
$Os(ttp)_2^{2+}$	+0.89				−1.17[b]
MV^{2+}				−0.44[c]	
MePTZ			+0.74[d]		
MeDPAA		+0.65[e]			
PTZ–$Os(ttp)_2^{2+}$	+0.90		+0.76		−1.19
DPAA–$Os(ttp)_2^{2+}$	+0.94	+0.76			−1.24
$Os(ttp)_2^{2+}$-MV^{2+}	+0.90			−0.35	−1.20
PTZ–$Os(ttp)_2^{2+}$–MV^{2+}	+0.94		+0.78	−0.37	−1.17
DPAA–$Os(ttp)_2^{2+}$–MV^{2+}	+0.94	+0.75		−0.48	−1.21

[a] Acetonitrile solution, 298 K; $E_{1/2}$ values in V, vs SSCE. [b] The reduction wave of the second ttp ligand occurs at more negative potentials. [c] $E_{1/2} = -0.40$ V vs Ag/AgCl;[18] the reduction potential for the ttp–MV^{2+} moiety is −0.36 V. [d] $E_{1/2} = +0.40$ V vs Ag/Ag^+;[19] the reduction potential for the ttp–PTZ^+ moiety is +0.79 V. [e] Methyldi-*p*-anisylamine;[20] the reduction potential for the ttp–$DPAA^+$ moiety is +0.74 V.

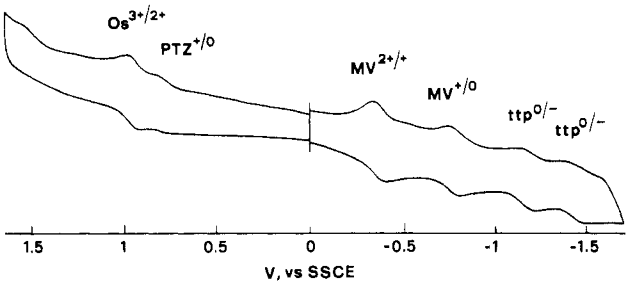

Figure 2. Cyclic voltammogram for the PTZ–$Os(ttp)_2^{2+}$–MV^{2+} triad.

Table II. Ground-State Absorption Maxima[a]

	λ_{max}, nm (ϵ, M^{-1} cm^{-1})			
$Os(ttp)_2^{2+}$	286 (58 000)	314 (68 000)	490 (26 000)	667 (6600)
$Os(ttp)_2^{2+}$–MV^{2+},[c]	285 (68 000)	315 (61 000)	490 (23 000)	668 (5700)
PTZ-$Os(ttp)_2^{2+}$	286 (68 000)	314 (75 000)	490 (28 000)	668 (7100)
DPAA-$Os(ttp)_2^{2+}$	285 (53 000)	314 (70 000)	503 (31 000)	671 (7800)
PTZ-$Os(ttp)_2^{2+}$–MV^{2+}	287 (66 000)	315 (56 900)	491 (24 000)	669 (6700)
DPAA-$Os(ttp)_2^{2+}$–MV^{2+}	280 (81 000)	314 (79 000)	504 (40 000)	672 (9200)

[a] Acetonitrile solution, 298 K.

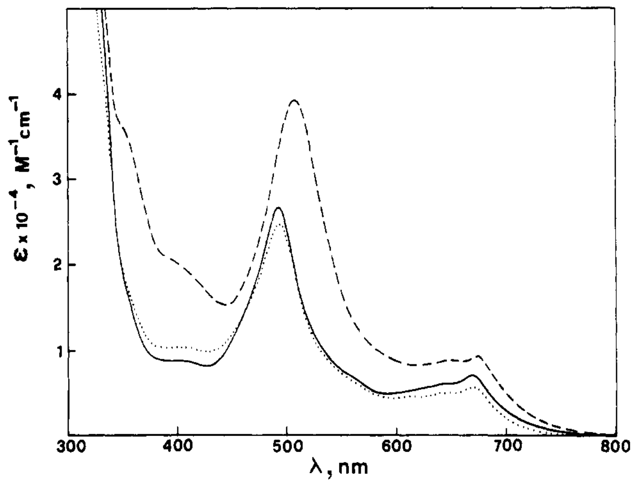

Figure 3. Absorption spectra of $Os(ttp)_2^{2+}$ (solid line), $Os(ttp)_2^{2+}$–MV^{2+} (dotted line), and DPAA–$Os(ttp)_2^{2+}$–MV^{2+} (dashed line).

Table III. Absorption Maxima of Some Oxidized and Reduced Components[a]

	λ_{max}, nm (ϵ, M^{-1} cm^{-1})		
$Os(ttp)_2^{3+}$	407 (22 700)	523 (5450)	618 (3950)
$Os(ttp)_2^{3+}$–MV^{2+}	404 (20 100)	517 (5250)	616 (3130)
MV^{+} [b]	397 (41 800)		607 (13 900)
ttp–$DPAA^{+}$ [c]	370 (14 000)	570 (4500)	740 (26 000)
*$Os(ttp)_2^{2+}$ [d]	390 (16 000)	430 (21 000)	600 (9000)

[a] Obtained by oxidation with Ce(IV) in $CH_3CN/HClO_4$ (4:1). [b] In CH_3CN.[22] [c] Reference 12. [d] Values estimated from the maxima of the room-temperature transient spectrum.

Table IV. Luminescence Data[a]

	298 K				155 K			
	λ, nm	τ, ns	I_{rel}[b]	τ_{CS}, ns	λ, nm	τ, ns	I_{rel}[b]	τ_{CS}, ns
$Os(ttp)_2^{2+}$	734	220	100		740	540	232	
PTZ–$Os(ttp)_2^{2+}$	734	220	98					
DPAA–$Os(ttp)_2^{2+}$	743	190	75					
$Os(ttp)_2^{2+}$–MV^{2+} [c]	738	0.26	1.2	d	745	4	4.5	27
DPAA–$Os(ttp)_2^{2+}$–MV^{2+} [c]	747	0.19	~1	d	755			d

[a] Solvent butyronitrile. Uncertainties: ±8% on lifetimes, ±10% on intensities. [b] The reported values are referred to the room temperature emission intensity of $Os(ttp)_2^{2+}$ taken as 100. Under such conditions, the luminescence quantum yield of $Os(ttp)_2^{2+}$ is 2.1×10^{-2} by comparison with $Os(bpy)_3^{2+}$ ($\phi_{em} = 5. \times 10^{-3}$, ref 15). [c] No quenching of the luminescence is observed in frozen solvent, i.e. at 77 and 90 K. [d] Not detected. Estimated lifetime ≤ 10 ns.

D and A components do not absorb in the visible region. Inspection of Table II reveals that the energy and the intensity of the CT transitions are hardly affected by the attached MV^{2+} and PTZ groups. In the case of DPAA, however, the energy and intensity of the CT bands show some minor change with respect to the isolated photosensitizer and the other systems. The absorption spectra of $Os(ttp)_2^{2+}$, $Os(ttp)_2^{2+}$–MV^{2+}, and DPAA–$Os(ttp)_2^{2+}$–MV^{2+} are shown in Figure 3.

In order to contribute to the elucidation of the transient spectra (vide infra), we have recorded the spectra of $Os(ttp)_2^{3+}$ and $Os(ttp)_2^{3+}$–MV^{2+} obtained by chemical oxidation of the corresponding Os(II) species. The absorption maxima of these spectra are collected in Table III, together with the maxima of MV^+,[22] ttp–$DPAA^+$,[12] and *$Os(ttp)_2^{2+}$.

Luminescence Properties. The $Os(ttp)_2^{2+}$ photosensitizer, P, is luminescent in the temperature range investigated (77–298 K). Both the luminescence intensity and lifetime decrease with increasing temperature (Table IV, Figure 4), with a pronounced discontinuity in the rigid–fluid transition temperature of the matrix.

The temperature dependence of the luminescence lifetime of the photosensitizer is shown in Figure 4. Least-squares fitting analysis of the experimental data according to eq 1[23] yielded the

$$1/\tau = k_0 + A_1 \exp(-\Delta E_1/RT) + A_2 \exp(-\Delta E_2/RT) \qquad (1)$$

following values for the various parameters: $k_0 = 3 \times 10^5$ s^{-1}, $A_1 = 7.5 \times 10^6$ s^{-1}, $\Delta E_1 = 210$ cm^{-1}, $A_2 = 9.8 \times 10^8$ s^{-1}, and $\Delta E_2 = 1430$ cm^{-1}. In Figure 4, the curve fitting to the experimental points includes the glass-to-fluid temperature interval (110–120 K) by using empirical temperature dependent terms.[23]

At room temperature, a quenching effect of dioxygen on the luminescence intensity and lifetime was found with a value of $(2.9 \pm 0.3) \times 10^9$ M^{-1} s^{-1} for the quenching constant.

At room temperature, the PTZ–P and the DPAA–P dyads do not show any substantial quenching of the luminescence with respect to P (Table IV). Therefore such dyads have not been explored at $T < 298$ K. In particular, the PTZ–P dyad behaves

---

(22) Venturi, M.; Mulazzani, G. Q.; Hoffman, M. Z. *Radiat. Phys. Chem.* **1984**, *23*, 229.

(23) Juris, A.; Balzani, V.; Barigelletti, F.; Campagna, S.; Belser, P.; von Zelewsky, A. *Coord. Chem. Rev.* **1988**, *84*, 85.

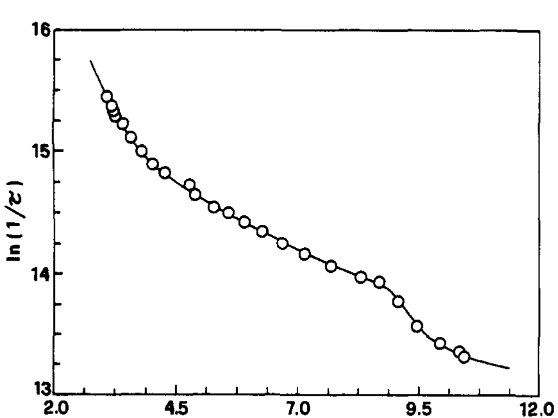

Figure 4. Temperature dependence of the emission lifetime for P in butyronitrile. τ is 220 ns and 1.7 μs at 298 and 90 K, respectively.

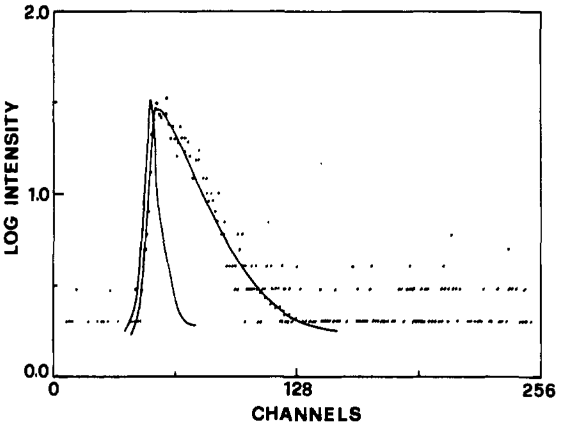

Figure 5. Luminescence decay of the P–MV^{2+} dyad at 298 K. The channel width is 16.4 ps. In the drawing the flash profile is also shown.

like the photosensitizer, whereas the DPAA–P dyad displays a slightly red-shifted luminescence spectrum and a slightly shorter lifetime.

For the P–MV^{2+} dyad, the luminescence properties in rigid matrix (77 and 90 K) are essentially the same as those of P. In fluid solution ($T > 150$ K), however, the luminescence intensity is almost completely quenched and the luminescence lifetime is very short (Table IV). Figure 5 shows the luminescence decay ($\tau = 260$ ps) of the P–MV^{2+} dyad at room temperature. The luminescence properties of PTZ–P–MV^{2+} (not reported in Table IV) and DPAA–P–MV^{2+} triads are essentially the same as those of the P–MV^{2+} dyad.

Transient Absorption Spectra. Laser flash-photolysis experiments were performed at 155 and 298 K in butyronitrile. Transient absorption spectra were recorded immediately after the 20-ns excitation pulse, and their decay was monitored at several wavelengths. The transient absorption spectra obtained at 155 K for the photosensitizer P and P–MV^{2+} dyad are shown in Figure 6.

The transient spectrum of the isolated photosensitizer at 155 K (Figure 6) shows bleachings in the 460–520- and 650–680-nm regions caused by the disappearance of the ground-state ^{1}MLCT and ^{3}MLCT bands. The positive absorptions at around 390, 600, and 750 nm can be assigned[12] to the reduced tpp$^-$ ligand, whereas the absorption around 430 nm, which is absent for the excited state of the analogous Ru(ttp)$_2{}^{2+}$ species,[12] is likely due to the intense LMCT band which is found at 407 nm in Os(ttp)$_2{}^{3+}$ (Table III). The transient spectrum decays with $\tau = 540$ ns at 155 K and 220 ns at room temperature, i.e., with the same lifetime values obtained for the luminescence decay.

For the P–MV^{2+} dyad, the transient spectrum recorded immediately after the flash at 155 K (Figure 6) is, at first sight, very similar to that of P. Its decay lifetime is 27 ns.

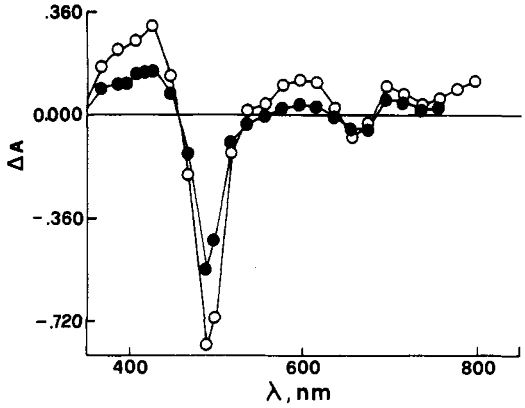

Figure 6. Transient difference absorption spectra, taken at 155 K at the end of the 20-ns laser pulse, for the photosensitizer P (○), and the P–MV^{2+} dyad (●). The absorbance at the excitation wavelength (532 nm) was 0.4.

The transient spectra of the PTZ–P and DPAA–P dyads do not show any sizable change with respect to that of P and decay to the ground state with lifetimes very close to that found for P. The behavior of the PTZ–P–MV^{2+} triad is identical to that of P–MV^{2+}.

The DPAA–P–MV^{2+} triad does not show any sizable transient absorption spectrum at 298 and 155 K. This indicates that the decay of the charge separated species takes place on a time scale comparable to, or faster than, the instrumental time resolution.

Discussion

Properties of the Isolated Photosensitizer. Within the usual[24,25] "localized" molecular-orbital approach, in the Os(ttp)$_2{}^{2+}$ photosensitizer one-electron oxidation is metal centered, one-electron reduction is ligand centered, and the low-energy absorption bands of Os(ttp)$_2{}^{2+}$ can be assigned to metal-to-ligand charge transfer (CT) transitions. Because of the large spin–orbit coupling, the absorption band corresponding to the triplet CT level ($\lambda_{max} \sim 670$ nm) displays a relatively high intensity (Table II). The luminescent level at low temperature is the lowest ^{3}CT level, which lies ~1.7 eV above the ground state. When the temperature is increased, two levels, lying at slightly higher energies (~200 and ~1400 cm^{-1}) than the lowest excited state, can be thermally populated, with a resulting moderate increase in the values of the radiative and nonradiative rate constants. Such upper levels are likely CT in nature.[26] Upper lying triplet metal-centered levels, which are responsible for the photodissociation reaction of the analogous Ru(II) complex,[23] cannot be reached because of the lower energy of the ^{3}CT level in the Os^{2+} complex and the higher ligand-field strength of Os^{2+} compared with Ru^{2+}. This accounts for the photochemical stability, the relatively long lifetime of the lowest excited state, and the luminescence exhibited by Os(ttp)$_2{}^{2+}$ in fluid solution at room temperature. The transient spectrum of Os(ttp)$_2{}^{2+}$ decays with the same lifetime of the luminescence, showing that it can be assigned to the ^{3}CT level.

Os(ttp)$_2{}^{2+}$ essentially maintains its spectroscopic and redox properties when it is covalently linked to MV^{2+} and/or PTZ to yield dyads and triads (Tables I, II, and IV). This can be explained in terms of the presence of the –CH$_2$– spacer between the components. On the contrary, DPAA is directly linked to the ttp ligand, and therefore it causes some perturbation in the electrochemical and spectroscopic properties.

Mechanism of the Photoinduced Processes. Approximate values for the energy of *P(^{3}CT) in the various supramolecular species (1.66 eV for the species containing DPAA, 1.69 eV for

---

(24) Crosby, G. A. *Acc. Chem. Res.* **1975**, *150*, 149.
(25) De Armond, M. K.; Carlin, C. M. *Coord. Chem. Rev.* **1981**, *36*, 325.
(26) Lumpkin, R. S.; Kober, E. M.; Worl, L. A.; Murtazza, Z.; Meyer, T. J. *J. Phys. Chem.* **1990**, *94*, 239.

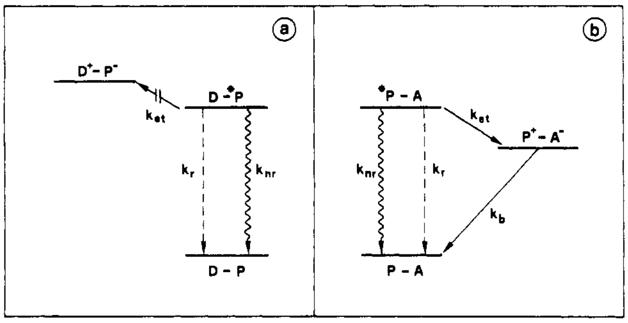

Figure 7. Schematic energy-level diagram for the D–P (a) and P–A (b) dyads.

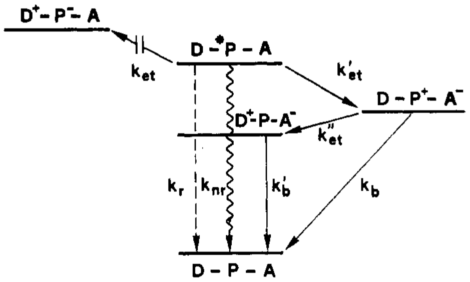

Figure 8. Schematic energy-level diagram for the D–P–A triads.

the other species) can be obtained from the maxima of the luminescence bands at 90 K. The energies of the charge-separated states can be evaluated from the potentials shown in Table I: $Os(ttp)_2^{3+}-MV^+$, 1.25 eV; $PTZ^+-Os(ttp)_2^+$, 1.95 eV; $DPAA^+-Os(ttp)_2^+$, 1.95 eV; $PTZ^+-Os(ttp)_2^{2+}-MV^+$, 1.11 eV; $DPAA^+-Os(ttp)_2^{2+}-MV^+$, 1.11 eV. The above values have to be considered as estimates rather than actual values, because of (i) the different conditions in which the electrochemical and spectroscopic data have been obtained and (ii) the different stabilization and Coulombic terms for the one-electron oxidized or reduced species and the charge-separated species.[5] Schematic energy level diagrams for the DPAA–P and $P-MV^{2+}$ dyads and the $DPAA-P-MV^{2+}$ triads are shown in Figures 7 and 8. It should also be noticed that MV^{2+}, PTZ, and DPAA do not exhibit any electronic excited state below 1.7 eV, so that in the dyads and triads energy transfer quenching cannot occur.

The behavior of the $PTZ-Os(ttp)_2^{2+}$ dyad, which was investigated only at room temperature, is the same as that of the isolated photosensitizer under all respects. This is an expected result since (i) the two components are isolated by a $-CH_2-$ group, and (ii) the charge-separated PTZ^+-P^- state lies at higher energy (1.95 eV) than the ^3CT excited state of the photosensitizer (1.69 eV) (Figure 7a).

As in the previous case, the charge-separated $DPAA^+-P^-$ level of the $DPAA-Os(ttp)_2^{2+}$ dyad lies at higher energy than the ^3CT level of the photosensitizer (Figure 7a). Therefore, quenching via the charge-separated state is not expected to occur. The small effects observed on luminescence intensity and lifetime (Table IV) are likely due to perturbation of the ^3CT level of the photosensitizer caused by the conjugation with DPAA. In this dyad, in fact, the two components are directly linked and perturbation effects can also be observed in the electrochemical and spectroscopic data (Tables I, II, and IV).

In the $Os(ttp)_2^{2+}-MV^{2+}$ dyad,[27] the charge-separated level lies at 1.25 eV, i.e., much below the ^3CT level of P (Figure 7b). A quenching of the photosensitizer luminescence via the charge-separated state can thus be expected. The results obtained (Table IV) show that about 99% of the luminescence intensity is indeed quenched, at both 298 and 155 K, whereas no quenching was observed, within the experimental uncertainty, in a rigid matrix (77 and 90 K). At room temperature the decrease in the luminescence lifetime is about 1 order of magnitude larger than the decrease in the luminescence intensity, suggesting that most of the residual emission is due to impurities (possibly, traces of P in $P-MV^{2+}$). In conclusion, the results obtained show that the excited photosensitizer in $P-MV^{2+}$ is quenched with rate constants 3.8×10^9 s^{-1} and 2.5×10^8 s^{-1} at 298 and 155 K, respectively. Since energy transfer quenching cannot occur in the $P-MV^{2+}$ dyad, there is no doubt that the observed quenching can be attributed to electron transfer quenching which, as shown in Figure 7b, is thermodynamically allowed in fluid solution. The lack of quenching in the rigid matrix further supports this conclusion. In a rigid matrix, in fact, solvent repolarization cannot occur so that the P^+-A^- state is destabilized by ~0.8 eV,[28] and the electronic transfer quenching process is expected to become endoergonic.

In spite of the close similarities of the transient spectra of $P-MV^{2+}$ and $^*P$, it can be safely excluded that the same species are observed in the two cases. In fact, the lifetime of $^*P$ in the dyad at 155 K, as determined by emission experiments, is 4 ns. Within the duration of the laser pulse (20 ns) the $^*P$ state has reacted to give a product which we identify as P^+-MV^+ (Figure 6).

The similarity between the transient spectra of $^*P$ and P^+-MV^+ is expected on the basis of the close similarity of the ttp^- and MV^+ spectroscopic properties.[12] At 155 K, a partial decay of the charge-separated species (τ = 27 ns) during the pulse (20 ns) can explain the decrease in ΔA of the transient spectrum in the case of the dyad compared to the chromophore (τ = 540 ns) without implying a lower than unity yield of charge-separated state and/or remarkable differences in the molar absorption coefficients. At room temperature, the luminescence state in the dyads (τ = 260 ps) is rapidly quenched but no charge-separated state is detected in the transient absorption experiments, indicating a rapid decay of the state (τ < 10 ns).

In conclusion the transient spectrum of the $P-MV^{2+}$ can be attributed to the P^+-MV^+ species which disappears via the back electron transfer reaction with rate $k_b = 3.7 \times 10^7$ s^{-1} at 155 K. The relatively low rate constant of the back electron transfer reaction compared to the forward reaction ($k_{et} = 2.5 \times 10^8$ s^{-1} at 155 K) is presumably related to a different electronic factor for the two reactions. In the forward reaction the electron transfer occurs from a tpp^- orbital to a MV^{2+} orbital, whereas the back reaction involves the transfer of an electron from the MV^{2+} π^* orbital to the t_{2g} metal orbitals. The back reaction could also marginally lie in the Marcus inverted region ($\Delta G°$ = −1.25 eV).

The behavior of the $PTZ-Os(ttp)_2^{2+}-MV^{2+}$ triad (Figure 8) is exactly the same as that of the $Os(ttp)_2^{2+}-MV^{2+}$ dyad, showing that the PTZ component does not affect the behavior of the photosensitizer and cannot be involved in fast electron transfer processes.

The behavior of the $DPAA-P-MV^{2+}$ triad can now be easily understood. The substantial difference of this system compared to that of the $P-MV^{2+}$ dyad lies in the presence of the low-energy D^+-P-A^- level. The decay of the excited photosensitizer is therefore almost unaffected; the small effect on the lifetime of $^*P$ on going from $^*P-MV^{2+}$ to $DPAA-{}^*P-MV^{2+}$, Table IV, is

---

(27) For recently investigated P–A systems containing viologen-like components see ref 12 and the following papers: (a) Yonemura, H.; Nakamura, H.; Matsuo, T. *Chem. Phys. Lett.* **1989**, *155*, 157. (b) Batteas, J. D.; Harriman, A.; Kanda, Y.; Mataga, N.; Nowac, A. K. *J. Am. Chem. Soc.* **1990**, *112*, 126. (c) Lin, J. X.; Yu, Q.; Zhou, Q. F.; Xu, H. J. *J. Chem. Soc., Chem. Commun.* **1990**, 260. (d) Shafirovich, V. Ya.; Amouyal, E.; Delaire, J. *Chem. Phys. Lett.* **1991**, *178*, 24. (e) Bierig, K.; Morgan, R. J.; Tysoe, S.; Gafney, H. D.; Strekas, T. C.; Baker, A. D. *Inorg. Chem.* **1991**, *30*, 4898. (f) Cooley, L. F.; Larson, S. L.; Elliott, C. M.; Kelley, D. F. *J. Phys. Chem.* **1991**, *95*, 10694. (g) Ryu, C. K.; Wang, R.; Schmehl, R. H.; Ferrere, S.; Ludwikow, M.; Merkert, J. W.; Headford, E. L.; Elliott, C. M. *J. Am. Chem. Soc.* **1992**, *114*, 430.

(28) Gaines, G. L., III; O'Neil, M. P.; Svec, W. A.; Niemczyk, M. P.; Wasielewski, M. R. *J. Am. Chem. Soc.* **1991**, *113*, 719.

likely due to an electronic perturbation of P by DPAA, as also shown by the absorption and luminescence spectra. The disappearance of the D–P^+–A^- species, however, can now occur not only via back electron transfer from A^- to P^+ (as in the case of the dyad) but also via the fully charge-separated D^+–P–A^- level (Figure 8). The process with rate constant k''_{et}, in fact, is expected to be very fast because it consists in the transfer of an electron from DPAA (which is strongly coupled with the photosensitizer) to the metal. The charge recombination reaction k'_b appears to be also very fast.

Conclusions

We have prepared five supramolecular systems (three dyads and two triads) based on the luminescent $Os(ttp)_2^{2+}$ photosensitizer (P), the electron donors PTZ and DPAA (D), and the electron acceptor MV^{2+} (A) (Figure 1), and we have studied their photoinduced processes. In a previous paper we studied the corresponding systems with P = $Ru(ttp)_2^{2+}$.[12] A comparison of the behavior of the two families of compounds may help to understand which factors play a role in determining the rates of the electron transfer processes. Since $Ru(ttp)_2^{2+}$ is very short lived and nonluminescent at room temperature, the systems based on that photosensitizer were investigated only at low temperature. The comparison will therefore be based on the behavior at 155 K where the lifetimes of the isolated photosensitizers are 4 μs ($Ru(ttp)_2^{2+}$) and 540 ns ($Os(ttp)_2^{2+}$).

For the PTZ–P and DPAA–P dyads, no electron transfer quenching is observed in the case of Os-based systems, as expected, because the process is noticeably endoergonic (Figure 7a). For the Ru-based systems, the process is only slightly endoergonic and some quenching in the case of the DPAA–P (where the electronic factor is certainly very favorable) has been observed.

For the P–MV^{2+} dyads, the electron transfer quenching leading to P^+–MV^+ is exoergonic in both cases (slightly more for the Os-based species), and luminescence quenching and flash experiments show that the process does take place (within 30 ns for the Ru dyad; with $k = 3.8 \times 10^9$ and 2.5×10^8 s^{-1} at 298 and 155 K, respectively, for the Os dyad).

There is a big difference, however, between the Ru and Os dyads as far as the fate of the P^+–MV^+ species is concerned. For the Os dyad, back electron transfer to the P–MV^{2+} ground state ($\Delta G^\circ = -1.25$ eV) takes place with $\tau = 27$ ns. For the Ru dyad, this process is apparently much slower (as expected because of its higher exoergonicity, $\Delta G^\circ = -1.63$ eV[12]), and the decay of the P^+–MV^+ species takes place only via the upper *P–MV^{2+} excited state (for other systems where the back reaction to the excited state prevails over the very exergonic back reaction to the ground state; see ref 29).

For both photosensitizers, the PTZ–P–MV^{2+} triads behave as the P–MV^{2+} dyad showing that the PTZ component, being isolated from P by a $-CH_2-$ spacer, does not play any role in the quenching of the excited photosensitizer. In the DPAA–P–MV^{2+} triads, however, where the DPAA component is directly conjugated to P, the presence of the electron donor makes the recovery of the ground state faster as compared with the P–MV^{2+} dyads. This is a likely consequence of the involvement of the fully charge-separated D^+–P–A^- state which undergoes fast charge recombination.

In order to have a longer lived D^+–P–A^- level, one or both of the following conditions should be satisfied: (i) a smaller electronic coupling between the electron donor and the photosensitizer (with a consequent smaller electronic coupling between electron donor and electron acceptor); (ii) a large exoergonicity of the charge recombination process (in order to be in the Marcus inverted region).

Acknowledgment. We thank P. Staub, L. Minghetti, and G. Gubellini for technical assistance. This work was supported by the Centre Nationale de la Recherche Scientifique and Ministere de la Recherche (France), and by the Programma Finalizzato Chimica Fine, Consiglio Nazionale delle Ricerche, and Ministero dell'Università e della Ricerca Scientifica e Tecnologica (Italy).

---

(29) Warman, J. M.; Smit, K. J.; de Haas, M. P.; Jonker, S. A.; Paddon-Row, M. N.; Oliver, A. M.; Kroon, J.; Oevering, H.; Verhoeven, J. W. *J. Phys. Chem.* **1991**, *95*, 1979.